



A Journal of the Gesellschaft Deutscher Chemiker

Angewandte Chemie

GDCh

International Edition

www.angewandte.org

Accepted Article

Title: Molecular, macromolecular, and supramolecular glucuronide prodrugs: an unexpected lead identified for anticancer prodrug monotherapy

Authors: Morten Jarlstad Olesen, Raoul Walther, Pier Poier, Frederik Dagnæs-Hansen, and Alexander N. Zelikin

This manuscript has been accepted after peer review and appears as an Accepted Article online prior to editing, proofing, and formal publication of the final Version of Record (VoR). This work is currently citable by using the Digital Object Identifier (DOI) given below. The VoR will be published online in Early View as soon as possible and may be different to this Accepted Article as a result of editing. Readers should obtain the VoR from the journal website shown below when it is published to ensure accuracy of information. The authors are responsible for the content of this Accepted Article.

To be cited as: *Angew. Chem. Int. Ed.* 10.1002/anie.201916124
Angew. Chem. 10.1002/ange.201916124

Link to VoR: <http://dx.doi.org/10.1002/anie.201916124>
<http://dx.doi.org/10.1002/ange.201916124>

COMMUNICATION

Molecular, macromolecular, and supramolecular glucuronide prodrugs: an unexpected lead identified for anticancer prodrug monotherapy

Morten T. Jarlstad Olesen^{a,b}, Raoul Walther^a, Pier Paolo Poier^a, Frederik Dagnæs-Hansen,^c
Alexander N. Zelikin^{a,b*}

Abstract: In this work, we perform tumor growth intervention via localized drug synthesis within the tumor volume, using the enzymatic repertoire of the tumor itself. Towards the overall success, we design molecular, macromolecular, and supramolecular glucuronide prodrugs for a highly potent toxin, monomethyl auristatin E (MMAE). The lead candidate exhibited a fold difference in toxicity between the prodrug and the drug of 175, had an engineered mechanism to enhance the deliverable payload to tumours, and contained a highly potent toxin such that bioconversion of few prodrug molecules created concentration of MMAE sufficient for efficient suppression of tumor growth. Each of these points is highly significant and together afford a safe, selective anticancer measure, making tumor-targeted glucuronides attractive for translational medicine.

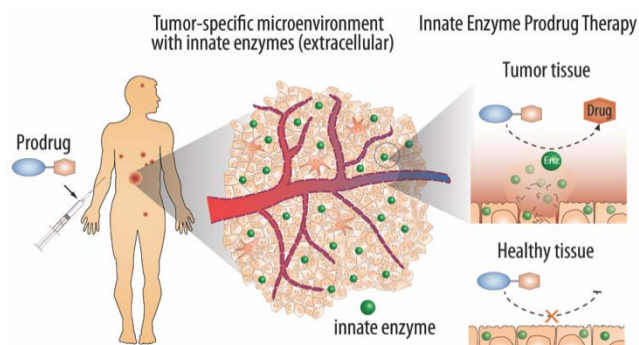
Systemic toxicity is the single most important determinant of success or failure of anticancer drugs. Side effects due to the systemic drug exposure exert the upper limit of the achievable plasma drug concentration, often well below the optimized *in vitro* dose. A powerful approach to overcome this is via a localized activation of prodrugs at the site of action.^[1] Such localized drug synthesis has been accomplished via the “enzyme prodrug therapies” (EPT) differed by the approach to localize the enzyme at the tumor site. Most notably, this has been accomplished using antibodies,^[2] localized gene expression,^[3] and/or via engineering enzymes into implantable biomaterials^[4]. An elegant, unique strategy for therapeutic cancer intervention lies in using the enzymatic repertoire of the tumor itself, via an innate, disease-mediated EPT (*i*-EPT, Scheme 1).^[5] The tumor microenvironment is rich in extracellular enzymes that in healthy tissues are confined to the intracellular compartments.^[6] This phenomenon provides a high specificity of enzyme localization in the body, for a highly localized prodrug activation.^[7]

Herein, we reveal that key to a successful *i*-EPT (cancer prodrug monotherapy) lies in maximizing the prodrug delivery to

the tumor. We focused on the privileged glucuronide scaffold^[8] and engineered molecular, macromolecular, and supramolecular prodrugs, advancing from the front-line methodologies in the fields of polymer therapeutics^[9] and albumin-based protraction methodologies^[5a, 10] (Figure 1A,B). All the designed prodrugs successfully masked the toxicity of the incorporated drug, and all prodrugs released the drug upon enzymatic bioconversion *in vitro*, but only one prodrug provided significant anticancer effect *in vivo*. The lead candidate could not be predicted based on existing literature reports, and could not be identified based on the *in vitro* toxicity screens. Results of this study are highly important in presenting a novel, superior scaffold for prodrug delivery to tumors. We believe that this scaffold will prove useful to all the diverse modalities of cancer detection, imaging, and treatment that rely on enhanced tumor localization of the administered (pro)drug.^[5a, 7]

Delivery of an enhanced injected dose to tumors can rely on the tools of active and/or passive targeting. Active, receptor-mediated targeting can be achieved using antibodies and small molecule conjugates, of which the former appear to be advantageous.^[11] However, active targeting is suited only to the well-characterized cancers with a documented phenotype. In turn, passive targeting is advantageous in that it relies on non-specific, broadly applicable methodologies of decreasing renal excretion of the injected dose, and/or the tumor-associated “enhanced permeation and retention” (EPR) effect, which together facilitate accumulation of the injected dose within the tumor.^[12]

Macromolecular^[9a] and supramolecular tools of nanomedicine^[13] are academically successful in their own right and present a wide landscape of opportunities for drug delivery via EPR. Of these, PEGylation is arguably the most successful synthetic methodology to produce macromolecular (pro)drugs



Scheme 1. Schematic illustration of the innate Enzyme Prodrug therapy (*i*-EPT).

[a] Dr. M.T. Jarlstad Olesen, Dr. R. Walther, P.P. Poier, Dr. A.N. Zelikin
Department of Chemistry, Aarhus University, Aarhus, Denmark
E-mail: zelikin@chem.au.dk

[b] Dr. M.T. Jarlstad Olesen, Dr. A.N. Zelikin
iNano Interdisciplinary Nanoscience Centre,
Aarhus University, Aarhus, Denmark

[c] F. Dagnæs-Hansen
Department of Biomedicine, Aarhus University, Aarhus, Denmark

Supporting information for this article is given via a link at the end of the document.

COMMUNICATION

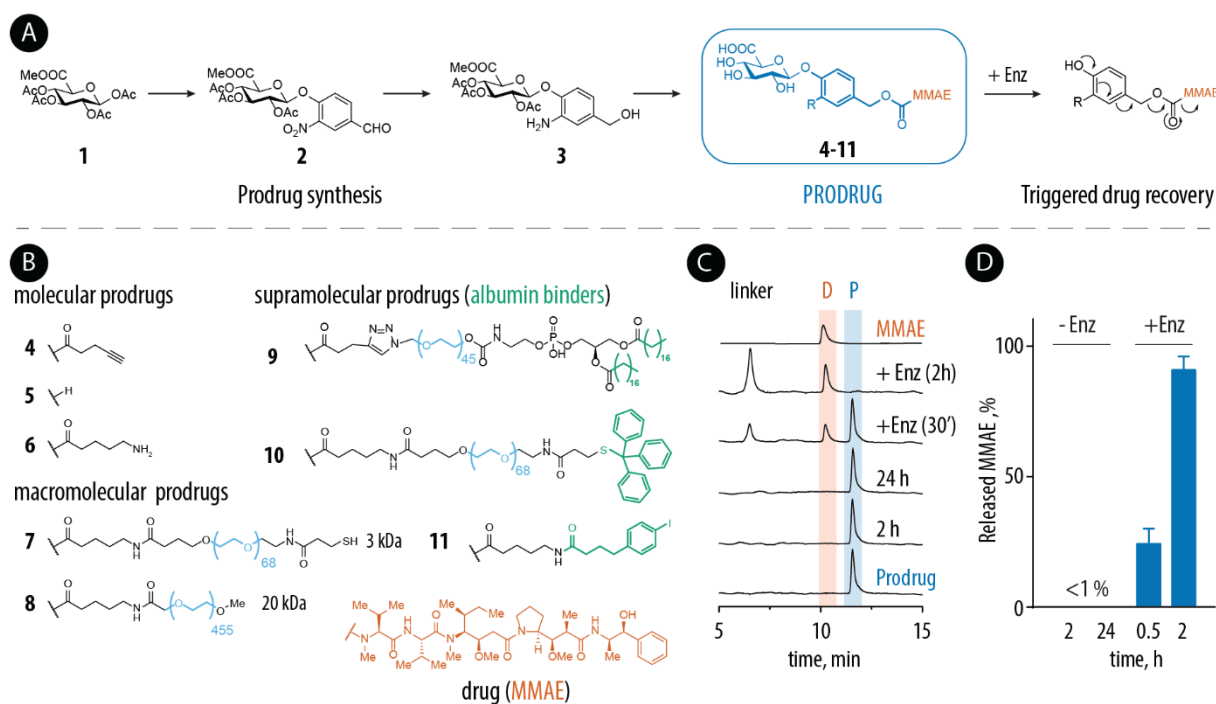


Figure 1. Prodrugs structures, synthesis scheme, and bioconversion. (A) Schematic illustration of the key synthetic steps in the synthesis of the prodrugs of MMAE employed in this work, and the mechanism of triggered release; For detailed synthetic procedures and compound characterization details, see supplementary materials; (B) Chemical structures of the protraction arm R in the structure of the prodrugs of MMAE; (C) normalized HPLC chromatograms for prodrug 4 (20 mg/L) illustrating prodrug stability upon incubation in phosphate buffered saline for a period of at least 24 h and drug recovery within 2 h of incubation in the presence of β -glucuronidase (1 mg/L) at 37°C; (D) Quantitative evaluation of the stability and hydrolysis of prodrug 4 in the presence or absence of β -glucuronidase from C, data represented as mean \pm SD of 3 independent experiments (N=3)

with optimized pharmacokinetics, for both biological [14] and small molecule [15] therapeutics. PEGylation serves to increase the hydrodynamic radius of the molecule, which leads to impede renal filtration, to limit non-specific tissue penetration, and to facilitate accumulation in tumors via the EPR effect. [16] An equally successful biological counterpart is albumin, the most abundant protein in human plasma, characterized with a phenomenal circulation half-life of around three weeks. [17] Drug conjugates [18] and supramolecular non-covalent adducts [10b] with albumin are successful in their own right, of which the latter are increasingly popular due to decreased handling of the biomolecule and the incredibly broad spectrum of synthetic opportunities to define affinity to albumin and the pharmacokinetics of the therapeutic molecule. [10a] Indeed, the overall majority of covalent conjugates to albumin pursue the same chemistry of maleimide-to-Cys34 conjugation. [19] In contrast, the arsenal of non-covalent binders contains dozens of ligands and spacers with associated opportunities to fine-tune pharmacokinetics of the (pro)drug. [10b, 20]

We engineered a library of molecular, macromolecular, and supramolecular prodrugs using a modular, self-immolative prodrug scaffold based on *o*-substituted *p*-hydroxybenzyl alcohol (PHBA) (Figure 1A). [21] This scaffold is unique in that it presents three sites of modification to install i) the effector molecule, ii) the trigger for drug release, and iii) the protraction arm. [5a] We focused on the glucuronide prodrugs due to their privileged position in EPT. [8] Glucuronides are well water-soluble and typically have restricted cell entry. The latter attribute endows glucuronides with the highest documented change in toxicity between the prodrug and the drug (i.e. QIC₅₀, calculated as a fold-ratio between the corresponding IC₅₀ values). [8] As a drug, we used monomethyl

auristatin E (MMAE), one of the most potent toxins used in medicinal practice. [22] Finally, the protraction arm R was introduced at a late stage of the synthesis and varied between PEG 2,000 Da and PEG 20,000 Da (tools of polymer therapeutics), as well as 1,2-distearoyl-*sn*-glycero-3-phosphoethanolamine (DSPE), 4-(*p*-iodophenyl)butyric acid (AlbuTag), and trityl group (Tr), of which the latter three are known albumin binders. [10b, 23]

Synthesis of prodrugs started from the commercially available 1,2,3,4-tetra-*O*-acetyl- β -D-glucuronide methyl ester **1** (Figure 1A and S11). First step included the formation of the extended scaffold [24] via chemical *O*-glycosylation of 4-hydroxy-3-nitrobenzaldehyde (**2**). [6c] Subsequently, the aldehyde functionality and the nitro group were reduced stepwise to the benzylic alcohol and an aniline (**3**), respectively. Acylation of aniline was then performed to introduce the alkyne or a primary amine functionality. Conjugation of the MMAE toxin was achieved with the use of 4-nitrophenyl chloroformate chemistry. [25] Finally, conjugation of the protraction arm R was developed as the late stage diversification, performed via either a direct reaction with activated esters or the copper catalysed azide-alkyne cycloaddition.

Using this general methodology, we obtained a total of eight prodrugs (**4-11**) with envisioned diversity of pharmacokinetic properties (Figure 1B). Molecular prodrugs (**4-6**) are simplest by structure, are highly water soluble, and are expected to have shortest blood residence time of the synthesized prodrugs. [26] Macromolecular prodrugs (**7-8**) are engineered via PEGylation, a strategy that limits renal excretion of the molecule by virtue of having an increased hydrodynamic radius and also enhanced tumor accumulation via the EPR effect. [16] Finally, supramolecular

COMMUNICATION

Table 1. Toxicity related IC₅₀ data for the glucuronide prodrugs against triple-negative human MDA-MB-231 breast adenocarcinoma cells in the absence or presence of β-glucuronidase (- Enz / + Enz, respectively). QIC₅₀ denotes the toxicity ratio between non-activated and enzyme activated prodrug: QIC₅₀ = IC₅₀ (- Enz) / IC₅₀ (+ Enz). Toxicity of MMAE in these experiments was 1.1±0.5 nM.

Prodrug R=	IC ₅₀ (- Enz)	IC ₅₀ (+ Enz)	QIC ₅₀
Alkyne (4)	255	0.6	425
H (5)	260	2.2	118
PEG _{3k} (7)	9.4	5.4	1.7
PEG _{20k} (8)	10.5	1.5	7
DSPE-PEG (9)	184	2.4	77
Tr-PEG (10)	579	3.3	175
AlbuTag (11)	1746	67.4	47

prodrugs (9-11) are designed such as to benefit from the beneficial pharmacokinetic characteristics of albumin, including extended blood residence time and potential increased tumor accumulation.^[18]

HPLC release studies revealed that all synthesized glucuronide prodrugs exhibit high stability in physiological buffer (phosphate buffered saline) for at least 24 h at 37°C, a feature that is highly important to minimize the non-specific drug release (Figure 1C and D and supplementary materials for the remaining prodrugs). All prodrugs released MMAE quantitatively in presence of β-glucuronidase, revealing that protraction arms R do not hinder enzymatic prodrug activation.

Cell culture evaluation of the prodrugs was conducted using highly metastatic triple-negative (oestrogen receptor (ER)-, progesterone receptor (PR)-, human epidermal growth factor receptor 2 (HER2) negative; claudin-low subtype) MDA-MB-231 human breast adenocarcinoma cells^[27] with limited treatment responsiveness (Figure S7 and Table 1). For each prodrug, toxicity was monitored in the presence or absence of the activating enzyme, allowing 72 h for the toxin to exert its effect. Under these conditions, over multiple independent runs, pristine MMAE revealed an IC₅₀ value of 1.1±0.5 nM. In agreement with their design, the extended scaffold glucuronides were significantly less toxic than MMAE whereas toxicity was restored via enzymatic bioconversion and ensuing drug release, with QIC₅₀ values as high as 425. Interestingly, prodrug structure and specifically the protraction arm R had a profound effect on the IC₅₀ of the prodrugs, their ability to undergo enzymatic bioconversion, and the resulting QIC₅₀ values. The first observation is that PEGylated prodrugs (7, 8), surprisingly, were the least effective in masking toxicity of MMAE and exhibited IC₅₀ values around 10 nM. Corresponding values for all other prodrugs, including the albumin-affine DSPE-PEG (9) and Tr-PEG (10), were well over 100 nM. PEGylation is a validated method to minimize translocation of drugs across biological membranes (e.g. Naloxegol is a PEGylated, peripherally active opioid).^[15] Apparent increase in toxicity for PEGylated glucuronides 7, 8 (compared to the simplified, parent prodrugs alkyne (4), R=H (5)) is therefore surprising. From a different perspective, our data demonstrate that all the prodrugs underwent efficient bioconversion, which resulted in the restored cytotoxicity of MMAE. However, the AlbuTag-functionalized glucuronide stands out as the prodrug with impeded bioconversion, as evidenced by a relatively high IC₅₀ = 67 nM observed for the prodrug in the presence of β-glucuronidase. A likely explanation to this is that AlbuTag is a relatively short spacer, in which case albumin creates a steric shield and hinders enzymatic activity on the prodrug. This effect was not observed for DSPE-PEG (9) or Tr-PEG (10) prodrugs for

which PEG presents a sufficient spacer between albumin and the glucuronic acid.

For successful *i*-EPT, the envisioned mechanism of prodrug bioconversion relies on the endogenous, rather than the externally administered enzyme. We verified if the enzymatic repertoire of the cancer cells is sufficient for prodrug bioconversion. Cancer xenografts based on triple-negative MDA-MB-231 breast adenocarcinoma cells were explanted from mice and incubated in PBS in the presence of resorufin-β-D-glucuronide (ResoGlcA), a fluorogenic probe employed such that increase in fluorescence intensity indicates enzymatic bioconversion of the probe. Explanted xenografts became well fluorescent when cultured in the presence ResoGlcA, providing an *ex vivo* validation of *i*-EPT (imaging modality) (Figures S7,10,11). This was also true in the case of xenografts based on non-invasive human breast adenocarcinoma MCF-7 cells (ER⁺, PR⁺, HER2⁻, luminal subtype A)^[27] and these too afforded reliable conversion of the fluorogenic glucuronide (Figures S7,10,11). Thus, *in vivo* grown cancerous tissue is capable of converting glucuronide prodrugs, which is the most important pre-requisite for the success of *i*-EPT.

In vivo anticancer effects mediated by the prodrugs were quantified in the subcutaneous (s.c.) MDA-MB-231 ectopic xenografts. We employed a once-weekly s.c. administration of the prodrugs in line with the growing understanding that this route of administration considerably decreases treatment costs while providing patient convenience (home vs hospital administration).^[28] Pristine MMAE, in agreement with prior reports on the subject,^[5a] proved to be highly toxic and exhibited no curative effects (Figure 2 A₁, B₁). Molecular prodrug (R=H, 5) significantly masked systemic toxicity of MMAE and was well tolerated, as evidenced by the survival rate and the body weight of mice, (Figure 2 A₁, B₁) but afforded no discernible anticancer effect (Figure 2 C₁, D₁). Same holds true for the majority of macromolecular (PEG_{3k} (7)) and supramolecular (DSPE (9), AlbuTag (11)) prodrugs tested in this work, and while toxicity of treatment was much improved over MMAE monotherapy, improvement in the therapeutic effect was not observed (Figure 2 C_{1,2}, D_{1,2}). This observation was rather surprising and indicates that otherwise successful tools of nanomedicine, such as DSPE-PEG,^[23a] PEG, and AlbuTag^[10b] failed to facilitate translocation of the glucuronide prodrugs to the tumor in sufficient quantities required for a successful *i*-EPT, at least with the chosen sparse drug administration schedule. Worthy of note, the prodrug with a PEG_{20k} (8) protraction arm exhibited statistically significant suppression of the tumor growth rate and this prodrug scaffold deserves further optimization.

Our study reveals an unexpected lead formulation that afforded statistically significant suppression of tumor growth, namely the Tr-PEG glucuronide prodrug 10 (Figure 3 C_{1,2}, D_{1,2}). The prodrug based on Tr-PEG (10) was highly active *in vivo* while its close analogue without an albumin binding group (R = PEG_{3k} (7)) was not, providing evidence that albumin binding is key to the observed anticancer effect. However, prodrugs based on DSPE-PEG (9) and AlbuTag (11), both albumin affine, were ineffective, signifying that albumin affinity as such is not sufficient for success. Our results, and those from others,^[10, 23a] suggest that albumin binders are not the same with regards to the *in vivo* performance of the resulting supramolecular adducts, be it for delivery of vaccines or anticancer drugs. Most importantly, it appears that *in vitro* toxicity screens fail to provide predictive knowledge and nominate *a priori* leads for *in vivo* evaluation. Specifically, in our

COMMUNICATION

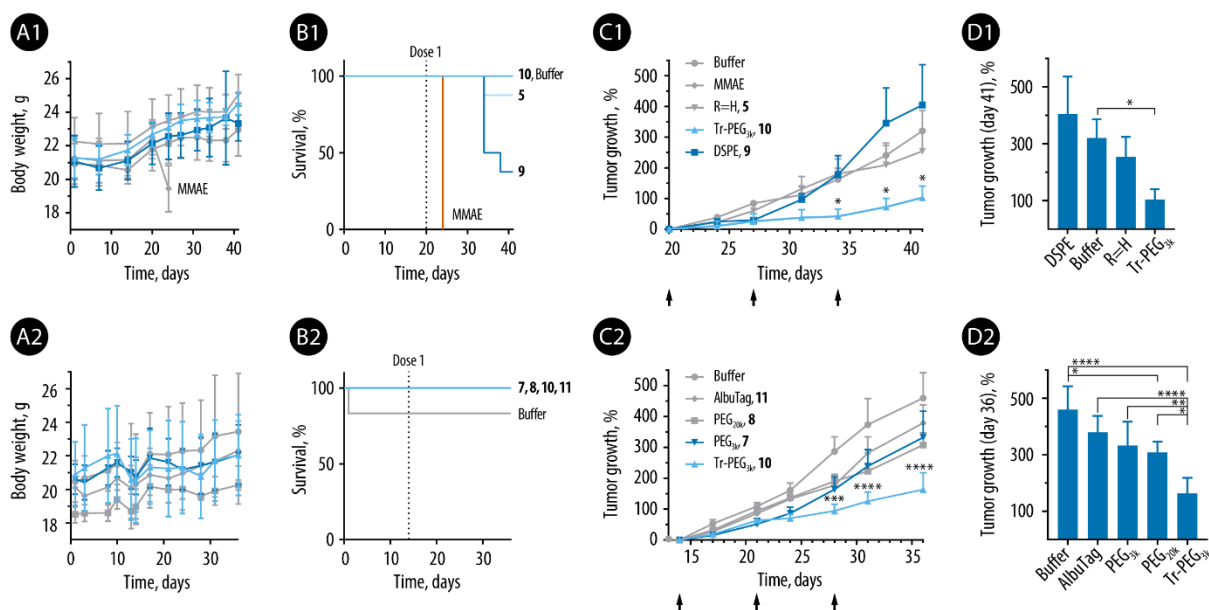


Figure 2. In vivo analysis of toxicity and anticancer activity revealed by the prodrugs of MMAE in ectopic human triple-negative MDA-MB-231 adenocarcinoma xenografts: (A_{1,2}) mice body weight; (B_{1,2}) Kepler-Meyer survival plots; (C_{1,2}) tumor growth data; (D_{1,2}) end-point statistical evaluation of the tumor growth at day 41 (D₁) or 36 (D₂). BALB/c-nu mice (n=8 (top panel) or n=6 (lower panel) per group) were inoculated s.c. with 3×10^6 MDA-MB-231 cells dorsally on the lower right flank. Arrows in panels C indicate drug administration (s.c., 1.5 mg/kg MMAE equivalents). Statistical significance was evaluated using a mixed-effects analysis (REML) followed by a Dunnett multiple comparisons test (C₁, D₁) or a two-way ANOVA followed by Tukey's multiple comparisons test (C₂, D₂). $P > 0.05$ (ns), $P \leq 0.05$ (*), $P \leq 0.01$ (**), $P \leq 0.001$ (***), $P \leq 0.0001$ (****). For panel C_{1,2} the asterisks indicate statistical comparison between Tr-PEG treated mice and buffer-dosed mice

hands, prodrugs that performed best *in vitro* (e.g. exhibited the highest QIC₅₀ or lowest toxicity of the non-activated prodrug) were not featured as leads after *in vivo* evaluation.

Next, we analyzed pharmacokinetics of selected prodrugs (based on PEG_{3k}, Tr-PEG, and DSPE-PEG). For this, imaging reagents were designed to contain the Cy7 fluorophore instead of the MMAE toxin. Imaging reagents were administered s.c., following which fluorescence was quantified in periodically collected blood samples. Characteristic blood content profiles (Figure 3A) were used to calculate the pharmacokinetics parameters (Table 2), specifically T_{max} (time to maximum plasma concentration), C_{max} (plasma concentration at maximum), AUC (area under curve), $T_{1/2 \beta}$ (plasma elimination half-life during the elimination phase), and K_{el} (elimination rate constant). Analysis of these data reveals that the imaging probe based on PEG_{3k} exhibited the highest T_{max} , C_{max} , and AUC, followed by the prodrug

based on Tr-PEG, which in turn was very similar to the DSPE-PEG counterpart. In other words, these pharmacokinetic parameters appear to hold no predictive value with regards to the anticancer effectiveness of the corresponding prodrugs of MMAE. However, we also observed that while the probe based on PEG_{3k} had the highest blood residence time, it was the counterpart based on Tr-PEG that exhibited the highest tumor accumulation, followed by probes based on PEG_{3k} and DSPE-PEG (Figure 3B). In our hands, tumor accumulation is the only pharmacokinetic parameter that shows correlation with the *in vivo* anticancer effects.

Analysis of the structure-activity relationship for the panel of molecular, macromolecular, and supramolecular prodrugs employed in this work reveals the Tr-PEG protraction arm to be the most effective tool to achieve enhanced tumor localization of the prodrug with ensuing tumor growth suppression. The likely mechanism of this pharmacokinetic phenomenon is that this prodrug associates non-covalently with albumin, as is the case for the DSPE and AlbuTag counterpart.^[10b, 28] However, affinity of trityl group to albumin to this point a conjecture as only limited prior art exists to support this notion.^[29] In an effort to validate such affinity, we performed *in silico* molecular docking simulations for albumin binding with trityl thioether as well as a panel of other known albumin binders, and considered two major ligand binding sites for albumin (the so-called Sudlow I and II sites). Computer modelling revealed no docking for trityl thioether to Sudlow II site. In stark contrast, docking to Sudlow I site was successful, with a docking score similar to a known Sudlow I binder indomethacin (for numerical values, see Tables S5 and S6). Docking simulations suggest that trityl ether binds such that it essentially superimposes with the most well-characterized Sudlow I ligands (which also give the lowest docking score, that is, have highest computed affinity), namely

Table 2. Pharmacokinetic parameters for the imaging probes containing PEG_{3k} ± Tr or DSPE-PEG protraction arm and Cy7 as an imaging fluorophore (n=4). BALB/cJRj mice were injected in the scruff with 0.4 mg/kg Cy7 labelled DSPE or PEG_{3k} ± Tr in a fluorescently matched dose. Buffer containing 4.8% DMSO was administered as control. Cy7 signal was analyzed over time from the plasma fraction of blood samples taken from the tail at the indicated time points.

Data refers to	agent	AUC _{5min-96h} (a.u.)	C _{max} (a.u.)	T _{max} (h)	K _{el} (h ⁻¹)	T _{1/2 β} (h)
Fig. 3A	DSPE-Cy7	0.9	4.61	2	0.029	24.2
Fig. 3A	PEG-Cy7	2.3	8.82	5	0.044	15.9
Fig. S12B	Tr-PEG-Cy7	0.58	3.78	2	0.047	14.7
Fig. S12B	PEG-Cy7	1.25	4.95	5	0.046	15.0

COMMUNICATION

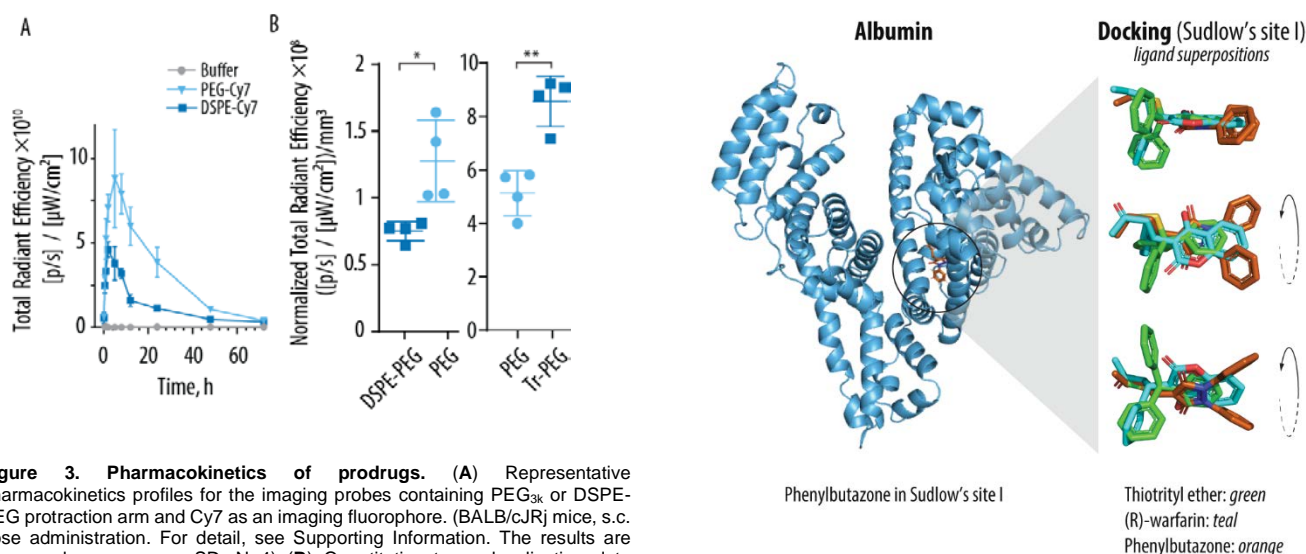


Figure 3. Pharmacokinetics of prodrugs. (A) Representative pharmacokinetics profiles for the imaging probes containing PEG_{3k} or DSPE-PEG protraction arm and Cy7 as an imaging fluorophore. (BALB/cJRj mice, s.c. dose administration. For detail, see Supporting Information. The results are expressed as means \pm SD, N=4) (B) Quantitative tumor localization data obtained in two consecutive experiments for pairwise comparison of PEG_{3k} with DSPE-PEG and PEG_{3k} and Tr-PEG (BALB/c-nu mice, MDA-MB-231 xenografts s.c. dose administration. For detail, see Supporting Information. The results are represented as means of quadruplets \pm SD (n = 4). Statistical significance was evaluated using an unpaired t-test. $P \leq 0.05$ (*), $P \leq 0.01$ (**).

phenylbutazone and warfarin, Figure 4. Thus, computer simulations strongly suggest that trityl ether is a good albumin binder, likely endowing the conjugated cargo with albumin hitchhiking property *in vivo*.

Taken together, this study is important in that we designed and compared side-by-side molecular, macromolecular, and supramolecular glucuronide prodrugs for MMAE to achieve localized, autonomous bioconversion within the tumor volume with ensuing cancer growth suppression. All prodrugs significantly masked toxicity of MMAE, as observed both *in vitro* and *in vivo*, and all prodrugs released MMAE upon bioactivation. Remarkably, significant variations were observed with regards to IC₅₀ and QIC₅₀ for the prodrugs *in vitro*, and even greater difference was observed *in vivo*, in which case only two prodrugs exhibited statistically significant cancer growth suppression and one formulation stood out as a lead. The identified lead could not be predicted from the *in vitro* toxicity screens or *in vivo* derived pharmacokinetics parameters (total drug exposure AUC, C_{max}, T_{max} and plasma half-life T_{1/2}β). When comparing imaging probes and anticancer prodrugs with the same protraction arm, we find that anticancer effects correlate only with one other parameter, namely extent of the tumor localization of the probe.

From a translational perspective, we believe that the designed prodrugs offer several decisive points of advantage. First, glucuronide conversion within the tumor volume has recently been shown to be a highly specific process, so much so that it can be used for cancer detection⁷, illustrating inherent safety of cancer prodrug monotherapy with the use of glucuronides. In turn, the QIC₅₀ values we record for glucuronides are significantly higher than those for e.g. hypoxia activated prodrugs (HAP) that were evaluated and failed in multiple clinical trials^[30] (QIC₅₀ under 10 for HAP, over 175 for the lead candidate engineered in this work). In other words, our prodrugs are significantly more selective and safer. Furthermore, prodrugs developed in this work have an engineered mechanism to enhance the deliverable payload to tumors, further contributing to the safety of this platform. Finally, in stark contrast with micromolar potency of HAP, doxorubicin and many other

Figure 4. Computational modelling of binding between albumin and ligands. Structure of albumin co-crystallized with phenylbutazone (orange) (PDB code: 2BXC) binding to Sudlow's site I (left side). Superpositions of phenylbutazone (orange), (R)-warfarin (teal) and methyl trityl thioether (green) are presented in their putative binding mode to Sudlow's site I and displayed from three different angles (right side). For SP values (docking scores), see Table S5 (Sudlow's site I) and Table S6 (Sudlow's site II).

anticancer drugs, MMAE is phenomenally potent such that bioconversion of few prodrug molecules creates the concentration of MMAE sufficient for efficient cell killing - and with a pronounced by-stander effect to affect the tumor volume. Each of these points is significant and together, these attributes render tumor targeted glucuronides attractive for translational studies. We are now optimizing drug dose and administration frequency to optimize the anticancer effects.

Acknowledgements. ANZ acknowledges funding from the European Research Council Consolidator Grant (ERC-2013-CoG 617336 BTVI); PPP acknowledges Danish Council for Independent Research (Grant No. 4181-00030).

References

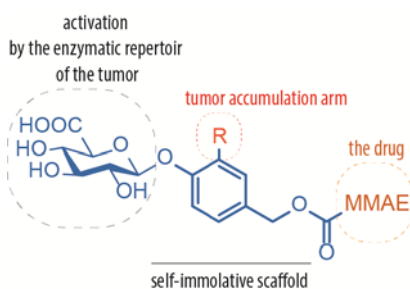
- [1] B. Städler, A. N. Zelikin, *Adv. Drug Deliv. Rev.* 2017, 118, 1.
- [2] S. K. Sharma, K. D. Bagshawe, *Adv. Drug Deliv. Rev.* 2017, 118, 2-7.
- [3] R. Mooney, A. Abdul Majid, J. Batalla, A. J. Annala, K. S. Aboody, *Adv. Drug Deliv. Rev.* 2017, 118, 35-51.
- [4] a) B. Fejerskov, M. T. Jarlstad Olesen, A. N. Zelikin, *Adv. Drug Deliv. Rev.* 2017, 118, 24-34; b) M. T. J. Olesen, A. K. Winther, B. Fejerskov, F. Dagnaes-Hansen, U. Simonsen, A. N. Zelikin, *Adv. Therap.* 2018, 1, 1800023.
- [5] a) Renoux, F. Raes, T. Legigan, E. Peraudeau, B. Eddhif, P. Poinot, I. Tranoy-Opalinski, J. Alsarraf, O. Koniev, S. Kolodych, S. Lerondel, A. Le Pape, J. Clarhaut, S. Papot, *Chem. Sci.* 2017, 8, 3427-3433; b) S. Cazzamalli, B. Ziffels, F. Widmayer, P. Murer, G. Pellegrini, F. Pretto, S. Wulhfard, D. Neri, *Clin. Cancer Res.* 2018, 24, 3656-3667.
- [6] a) B. Sperker, J. T. Backman, H. K. Kroemer, *Clin. Pharmacol.* 1997, 33, 18-31; b) D. Weyel, H. H. Sedlacek, R. Müller, S. Brüsselbach, *Gene Ther.* 2000, 7, 224; c) K. Bosslet, R. Straub, M. Blumrich, J. Czech, M. Gerken, B. Sperker, H. K. Kroemer, J.-P. Gesson, M. Koch, C. Monneret, *Cancer Res.* 1998, 58, 1195-1201.

COMMUNICATION

- [7] a) A. N. Zelikin, *Nat. Chem.* **2019**, doi: 10.1038/s41557-019-0400-0; b) J. Lange, B. Eddhif, M. Tarighi, T. Garandeau, E. Péraudeau, J. Clarhaut, B. Renoux, S. Papot, P. Poinot, *Angew. Chem. Int. Ed.* **2019**, *58*, 17563-17566.
- [8] R. Walther, J. Rautio, A. N. Zelikin, *Adv. Drug Deliv. Rev.* **2017**, *118*, 65-77.
- [9] a) I. Ekladios, Y. L. Colson, M. W. Grinstaff, *Nat. Rev. Drug Discov.* **2019**, *18*, 273-294; b) C. F. Riber, A. N. Zelikin, *Curr. Op. Coll. Interf. Sci.* **2017**, *31*, 1-9.
- [10] a) J. Lau, P. Bloch, L. Schaffer, I. Pettersson, J. Spetzler, J. Kofoed, K. Madsen, L. B. Knudsen, J. McGuire, D. B. Steensgaard, H. M. Strauss, D. X. Gram, S. M. Knudsen, F. S. Nielsen, P. Thygesen, S. Reedt-Runge, T. Kruse, *J. Med. Chem.* **2015**, *58*, 7370-7380; b) J. Lau, O. Jacobson, G. Niu, K.-S. Lin, F. Bénard, X. Chen, *Bioconj. Chem.* **2019**, *30*, 487-502.
- [11] S. Cazzamalli, A. Dal Corso, F. Widmayer, D. Neri, *J. Am. Chem. Soc.* **2018**, *140*, 1617-1621.
- [12] S. K. Golombek, J. N. May, B. Theek, L. Appold, N. Drude, F. Kiessling, T. Lammers, *Adv. Drug Deliv. Rev.* **2018**, *130*, 17-38.
- [13] J. Nam, S. Son, K. S. Park, W. Zou, L. D. Shea, J. J. Moon, *Nat. Rev. Mater.* **2019**.
- [14] A. N. Zelikin, C. Ehrhardt, A. M. Healy, *Nat. Chem.* **2016**, *8*, 997.
- [15] K. P. Garnock-Jones, *Drugs* **2015**, *75*, 419-425.
- [16] R. B. Greenwald, Y. H. Choe, J. McGuire, C. D. Conover, *Adv. Drug Deliv. Rev.* **2003**, *55*, 217-250.
- [17] J. T. Sockolosky, F. C. Szoka, *Adv. Drug Deliv. Rev.* **2015**, *91*, 109-124.
- [18] L. Pes, S. D. Koester, J. P. Magnusson, S. Chercheja, F. Medda, K. Abu Ajaj, D. Rognan, S. Daum, F. I. Nollmann, J. Garcia Fernandez, P. Perez Galan, H. K. Walter, A. Warnecke, F. Kratz, *J. Controlled Release* **2019**, *296*, 81-92.
- [19] B. Elsadek, F. Kratz, *J. Controlled Release* **2012**, *157*, 4-28.
- [20] C. Müller, R. Farkas, F. Borgna, R. M. Schmid, M. Benešová, R. Schibli, *Bioconj. Chem* **2017**, *28*, 2372-2383.
- [21] P. L. Carl, P. K. Chakravarty, J. A. Katzenellenbogen, *J. Med. Chem.* **1981**, *24*, 479-480.
- [22] P. D. Senter, E. L. Sievers, *Nat. Biotechnol.* **2012**, *30*, 631.
- [23] a) H. Liu, K. D. Moynihan, Y. Zheng, G. L. Szeto, A. V. Li, B. Huang, D. S. Van Egeren, C. Park, D. J. Irvine, *Nature* **2014**, *507*, 519-522; b) W. Liu, J. Nie, X. Tan, H. Liu, N. Yu, G. Han, Y. Zhu, F. A. Villamena, Y. Song, J. L. Zweier, Y. Liu, *The Journal of Organic Chemistry* **2017**, *82*, 588-596; c) Y. Song, Y. Liu, C. Hemann, F. A. Villamena, J. L. Zweier, *J. Org. Chem.* **2013**, *78*, 1371-1376.
- [24] R. Walther, M. T. Jarlstad Olesen, A. N. Zelikin, *Org. Biomol. Chem.* **2019**, *17*, 6970-6974.
- [25] B. Sammet, *Synlett* **2009**, *2009*, 3050-3051.
- [26] A. V. Stachulski, X. Meng, *Nat. Prod. Reports* **2013**, *30*, 806-848.
- [27] Y. L. Liu, C. K. Chou, M. Kim, R. Vasisht, Y. A. Kuo, P. Ang, C. Liu, E. P. Perillo, Y. A. Chen, K. Blocher, H. Horng, Y. I. Chen, D. T. Nguyen, T. E. Yankeelov, M. C. Hung, A. K. Dunn, H. C. Yeh, *Sci. Rep.* **2019**, *9*.
- [28] A. C. Anselmo, Y. Gokarn, S. Mitragotri, *Nat. Rev. Drug Discov.* **2018**, *18*, 19.
- [29] Y. Song, Y. Liu, W. Liu, F. A. Villamena, J. L. Zweier, *RSC Adv.* **2014**, *4*, 47649-47656.
- [30] W. R. Wilson, M. P. Hay, *Nat. Rev. Cancer* **2011**, *11*, 393-410.

COMMUNICATION

Entry for the Table of Contents



Safe, tumor-accumulating prodrugs that are specific to the enzymatic repertoire of the tumor comprise an effective anticancer therapy. The lead structure could not be predicted by the in vitro / ex vivo screens but was identified through in vivo monitoring